LOW TEMPERATURE SPECTROSCOPY OF SOME TRANSITION METAL COMPOUNDS

THE DETERMINATION AND INTERPRETATION OF THE OPTICAL SPECTRUM OF CHROMIUM (III) TRIS-ACETYLACETONATE

by

Ray V. Work, Jr.

A Thesis Submitted to the Faculty of the

DEPARTMENT OF CHEMISTRY

In Partial Fulfillment of the Requirements
For the Degree of

MASTER OF SCIENCE

In the Graduate College

THE UNIVERSITY OF ARIZONA

1961

STATEMEMT BY AUTHOR

This thesis has been submitted in partial fulfillment of requirements for an advanced degree at the University of Arizona and is deposited in the University Library to be made available to borrowers under rules of the Library.

Brief quotations from this thesis are allowable without special permission, provided that accurate acknowledgment of source is made. Requests for permission for extended quotation from or reproduction of this manuscript in whole or in part may be granted by the head of the major department or the Dean of the Graduate College when in their judgment the proposed use of the material is in the interests of scholarship. In all other instances, however, permission must be obtained from the author.

SIGNED: Ray V. Wolf, Jr.

APPROVAL BY THESIS DIRECTOR

This thesis has been approved on the date shown below:

L. S. Forster — 5/19/61

L. S. Forster
Associate Professor of Chemistry

Date

ACKNOWLEDGMENTS

The author should like to express his sincere thanks to Dr. L. S. Forster, without whose guidance, assistance and patience, this project and thesis could not have been completed. The author also wishes to express his thanks to Dr. R. L. DuBois for his aid in the orientation of crystals for this study and to Dr. D. S. Chapin for his aid in the preparation of liquid helium for the low temperature studies made in this project.

TABLE OF CONTENTS

LIST OF ILLUSTRATIONS

LIST OF TABLES

ABSTRACT

The optical absorption spectrum of chromium (III) tris-acetylacetonate has been determined, using a grating spectrograph, at room temperature, 77°K and 4.2°K.

It is shown that, due to the similarity of the crystal field of this chelate to that of ruby, the optical absorption spectrum of this chelate may be interpreted using a previous interpretation of the ruby spectrum. The proposed assignments of the spectral features of $Cr(AcA)_3$ have been tentatively verified by a study of their optical anisotropy.

It is also shown that the position and spacing of the intercombination lines may be potentially useful as an indication of the degree of covalency of the metal-ligand bonds of chelates.

INTRODUCTION AND BACKGROUND

In 1929, Bethe[1] introduced the concept of the crystal field. He assumed that, in a complex of either the rare earths or the transition metals, the molecule could be treated as a central ion surrounded by 2, 3, 4, 5, 6 or more point charges. These point charges replaced the ligands of the complex, and their position and number were just the position and number of ligands.

He postulated that the energy levels of the central ion could be determined by assuming that these point charges created an electric field, which perturbed the various d or f orbitals, thus partially removing the degeneracy of these orbitals.

He formulated this problem mathematically and, using group theory, showed qualitatively how the different atomic states of the free atom would be affected by fields of different strength, due to the proximity of the ligands to the central ion, and of different symmetry, due to the number and location of the ligands.

The first use made of this theory was in 1932 by Schlapp and Penney[2], who used this electrostatic field concept to explain the magnetic behavior of complexes. Using this crystal field theory, they attempted to explain the changes in the paramagnetism of an ion when it is placed in a complex by calculating the paramagnetic susceptibility of several transition metal complexes. The expressions they obtained could be made to fit experimental values of the susceptibilities by assuming "reasonable values" for the parameters involved.

Very little was done with crystal field theory for the next twenty years. The existence of complexes as well as their magnetic properties could be explained, with a fair degree of accuracy, using Pauling's theory[3] of ionic and covalent bond types. Pauling's theory was also able to qualitatively rationalize many features of the optical spectra of complexes, since it led to reasonable conclusions about the positions of available energy levels, at least in the covalent complexes.

In 1952, however, Orgel[4] showed that crystal field theory was very similar to Pauling's concept of bonding types. There are essentially two types of complexes, differentiated by their magnetic behavior. The first, called ionic complexes by Pauling, exhibit the normal paramagnetism of the free ion. These are classed as weak field complexes in crystal field theory, in which it is assumed that the crystal field splitting is small compared to electronic repulsion, so that electrons will favor the higher energied orbitals rather than pairing in the already singly occupied lower energied orbitals. Thus an ion having four d electrons in a low field complex will have all four electrons with spins unpaired, resulting in the large magnetic moment exhibited by the free ion.

The second type of complexes are Pauling's covalent complexes, in which the paramagnetism observed in the free ion is reduced or destroyed. Using crystal field theory, this would be explained as a strong field case, where the crystal field splitting is larger than electron repulsion. Thus the electrons will favor pairing rather than promotion to one of the higher energy orbitals. Hence, an ion having six d electrons, which exhibits paramagnetism in the free state, will exhibit diamagnetism in an octahedral, strong field complex, due to a pairing of all six electrons in the three lower energied orbitals.

In this article, Orgel also showed qualitatively how crystal field theory could be used to explain heats of hydration of the transition metals. He showed that the anomalously low heats of hydration of Mn (II) and Fe (III) were due to a lack of crystal field stabilization, since both have S ground states, and hence are not stabilized by the formation of a crystal field.

Orgel also explained the deviation of many six-coordinated complexes from perfect octahedral symmetry in terms of a Jahn-Teller effect. Thus, using crystal field theory, the unusual stereochemistry of octahedral Cu (II) complexes, which have four short and two long bonds, can be explained. Pauling's covalent bonding theory could not explain this difference in the six metal-ligand bonds.

Since this revival of interest in crystal field theory in the early 1950s, a considerable amount of work has been published on applications of this theory. The greater part of this work has been attempts to better interpret the optical spectra of transition metal complexes.

Crystal field theory has been used to partially interpret the spectra of transition metal complexes as early as 1940.[5] However, these early studies were generally able to interpret qualitatively or semi-quantitatively only the broad, weak absorption bands characteristic of the optical spectra of these compounds. Many of the transition metal complexes exhibit, in addition to these bands, several sharp lines, or sets of lines, of very low intensity. Few of the early studies were able to interpret, even qualitatively, these lines. For a good review summarizing the work done on spectral interpretation prior to 1959, the reader is referred to McClure.[6]

The first good interpretation of large portions of these spectra was published in 1958 by Sugano and Tanabe.[7] In this work they interpreted the optical spectrum of ruby, which consists of small amounts of Cr (III) suspended in an aluminum oxide lattice. Since the Cr (III) presumably substitutes at the aluminum lattice sites, it is octahedrally surrounded by six oxygen atoms. Thus we may consider the ruby as a dilute, crystalline Cr (III) complex, the ligands being oxygen atoms.

In this study, the optical spectrum of Cr (III) tris-acetylacetonate, in the crystalline form, was examined at low temperatures. Since the Cr (III) of this chelate is octahedrally surrounded by six oxygen atoms, creating a field whose symmetry can be related to that of ruby, an attempt has been made to interpret this spectrum using Sugano and Tanabe's ruby interpretation. This study has been necessarily incomplete, but it is hoped that it may be indicative of the validity of this approach to the interpretation of the optical spectra of chelates.

CRYSTAL FIELD THEORY

Most of the physical and chemical properties of transition metal ions can be understood[8] from a study of ligand field theory, which is a grafting together of crystal field theory and molecular orbital bonding theory.

In electrostatic crystal field theory, the central metallic ion is considered to be subjected to an electric field, generated by the nearest atom of each ligand. This atom is usually either negatively charged or the negative end of an electric dipole.

This negative charge will repel the various d electrons of the central ion, the repulsion being greatest in the vicinity of the negative electrostatic charge. Since we presume the electronic distribution of d electrons to be characterized by five orbitals, the proximity of an orbital to the ligands will determine its destabilization by the crystal field. Thus the orbital degeneracy of the free ion is partially removed.

In a discussion of the effects of the crystal field, it is more meaningful to speak of the removal of the degeneracy of the atomic states, rather than discussing the effect of the field on electrons in the individual orbitals. This is most easily appreciated by remembering that an atom having one d electron cannot be considered as having an electron in one discrete orbital, but rather "one-fifth of an electron" in each of the five d orbitals. Thus it can be seen that a discussion of the orbital splitting is rather meaningless, except as an aid to an intuitive understanding of crystal field theory.

The manner in which a given atomic state splits is a function of the symmetry of the electrostatic field created by the ligands, as well as of the distance between the central ion and the ligands. Thus, in a perfectly octahedral field, an F state will split into three states, while in a distorted octahedral field, the degeneracy of the F state will be further removed by a splitting into six states.[6]

The relative energies of each component of a split state can, in theory at least, be calculated from perturbation theory. A potential fuction due to the field is assumed, which has the same symmetry as the field. A combination of atomic d orbitals is then chosen which exhibits the same symmetry as the split component under question. This potential function and this combination of atomic orbitals is then used in perturbation calculations to determine the energy of this component, relative to that of the atomic state from which it originates. The expressions obtained are difficult to solve and yield energy levels in terms of several parameters, which must be evaluated from the observed spectra.

In the study of octahedral complexes, the field is generally considered to have octahedral symmetry, either perfect or elongated along one axis. In the cases studied in this project, a trigonal field[7,9] is found to be superimposed on this octahedral field. This trigonal field has the effect of further splitting the components due to the octahedral field. As will be seen, this additional splitting gives rise to the optical anisotropy observed in the quartet-quartet transitions of the ruby.

Another effect needed to explain these spectra is that due to spin-orbit coupling. This coupling, which is neglected in the first approximation, is the interaction of the spin and the orbital angular momentum of an electron. The result of this coupling is to further split the energy levels of the doublet states in the presence of the crystal field. This splitting gives rise to the optical anisotropy observed in the quartet-doublet (intercombination) lines observed in these spectra.

The only other assumption needed in the interpretation of the spectrum of Cr (III) tris-acetylacetonate is the existence of covalent bonding. As is well known, if an atomic orbital is subjected to covalent bonding, molecular orbital formation, the energy of the resulting molecular orbital is lower than that of the original atomic orbital. Thus it may be said that covalent bonding lowers the energy of an atomic state.

EXPERIMENTAL TECHNIQUES

The tris-acetylacetonate chelates of Cr (III) and Co (III) were obtained from MacKenzie Chemical Works, Inc. and Electro Metallurgical Co. of Union Carbide Corp. The aluminum oxide boules, containing 0.06% and 1.8% Cr (III), were obtained from Linde Division of Union Carbide Corp. These boules were approximately two inches long by one-half inch in diameter.

The aluminum (III) tris-acetylacetonate, used to prepare mixed crystals, was prepared by mixing stoichiometric amounts of aluminum chloride and acetylacetone in an aqueous solution, made sufficiently alkaline with sodium hydroxide to dissolve any insoluble aluminum hydroxide formed. After stirring for five minutes at room temperature, the white, gelatinous precipitate of aluminum acetylacetonate was filtered, washed with water, and taken up in benzene. This method produced a large yield of pale yellow crystals.

The $Al(AcA)_3$ crystals were recrystallized from benzene and their visible absorption spectra determined, using a Cary Model 11 recording spectrophotometer. The absorption in the visible and near infared regions consisted of two small peaks at 430 mμ and 612.5 mμ, with molar extinction coefficients of 0.178 and 0.010 respectively. These were not intense enough to interfere with the work which was done with this compound, which was used as a transparent matrix for other chelates.

All compounds used in this study were purified by filtering benzene or ethanol solutions of the compound to remove any benzene or ethanol insoluble matter present. The chelate in solution was then recrystallized by boiling until saturated, cooling to room temperature or slightly below, and filtering out the precipitated chelate. The material thus obtained was used without further purification.

Since, for this work, large, thick crystals were not required, the usual methods of crystal growth were not used; i.e., seeding a supersaturated solution or slow, thermostatted cooling of a saturated solution. Other common techniques which were not applicable, due to the instability of the acetylacetonates to heat, include zone melting and growing from a melt.

It was found that two methods of crystal growth gave completely satisfactory crystals in three to four days. The first of these methods was the growth of the desired crystals directly on a beaker bottom by slow evaporation of a benzene or ethanol solution of the chelate. It was found that three or four grams of the desired chelate dissolved in seventyfive milliliters of solvent would produce a supply of usable crystals in three days.

For a study of the strongly absorbing transitions in materials whose crystalline structures were isomorphous with aluminum acetylacetonate, dilute, mixed crystals could be successfully grown. These were obtained by dissolving a known amount of the chelate under study in benzene with a known amount of $Al(AcA)_3$. This solution was then allowed to evaporate slowly, yielding mixed crystals whose concentration was known. Generally a ratio of ten to one hundred parts of the aluminum chelate per part of the transition metal chelate was used.

This technique will prove especially valuable for solid state studies of the more intense absorptions (e.g. ligand bands). It was generally found that for the forbidden transitions under study here, pure crystals of sufficient thinness could be prepared. The mixed crystals were used, however, for some studies of the 500-700 mμ region of the $Cr(AcA)_3$ spectrum.

The second crystal growth technique used was the growth of crystals at a benzene-water interface. The chelate was dissolved in benzene and this solution floated on a water layer. After the benzene had evaporated, well-formed crystals were lifted off the water, allowed to dry in air, and used. This method generally produced crystals of better size and shape with fewer visible surface defects than did the first method discussed. Using this technique minimized the danger of crystal breakage during removal of the crystals from the beaker. This technique is limited to water insoluble chelates. If, however, it were desired to use this on water soluble chelates, any liquid having the proper density, and in which the chelate and its solvent were insoluble, could be used.

The aluminum oxide boules were cut into useful pieces, using a diamond tipped saw, with one face parallel to the crystallographic c axis. The optical orientation was determined by means of a polarizing microscope. No attempt was made to cut or mount these boules with an accuracy greater than a one or two degree deviation in the position of the c axis.

For determination of the crystalline absorption spectra, the crystals were mounted on clear cellophane tape, which has no detectable absorption in the region 400-900 mμ. This tape was then mounted on a plastic holder painted black, with a small hole for the passage of light through the crystal. For a sketch of this holder, see Figure 1. This assembly was then placed in the inner compartment of a large, two compartment, vacuum jacketed dewar with optical windows. A long, removable plastic rod was used for adjustment and removal of the holder.

The dewar was mounted on a universal support which allowed precise adjustment of the dewar to compensate for changes in the length of the crystal holder on cooling. The dewar was attached to this universal support in such a way as to allow reproducible removal and replacement of the dewar.

For the 77°K studies, the inner compartment of the dewar was filled with liquid nitrogen and the crystal, which had been precooled with solid carbon dioxide, was placed in this liquid nitrogen

Fig. 1

EXPERIMENTAL APPARATUS

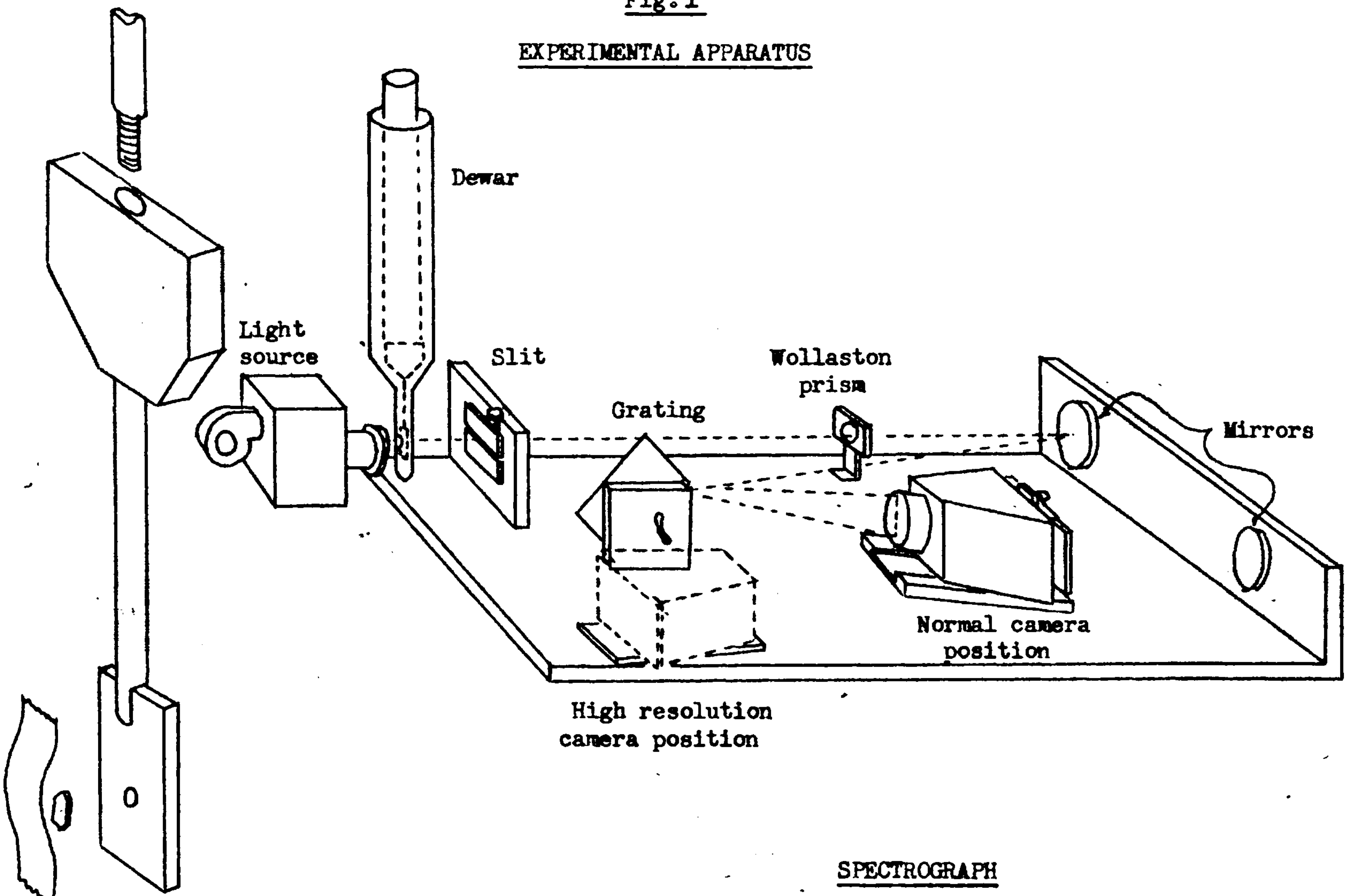

CRYSTAL HOLDER

SPECTROGRAPH

(with cover removed)

bath. This precooling of the crystal helped minimize thermal strain on the crystal due to rapid cooling by the liquid nitrogen.

For the 4.2°K studies, the outer compartment of the dewar was filled with liquid nitrogen to precool the dewar. The crystal was precooled as above and placed in the inner compartment which was then filled with liquid helium. It was found that liquid helium could be retained in the dewar for about one hour. It was found necessary to reduce the pressure in the vacuum jacket of the dewar to 10^{-5} mm Hg to prevent excessive condensation of air in this jacket on the optical windows of the dewar. This pressure reduction was accomplished with a mechanical vacuum forepump and a mercury diffusion pump.

The grating spectrograph used in this study was built for our group by Mr. Leon Solenave, of the University of Arizona. A sketch of this instrument is shown in Figure 1. The mirrors shown are concave, front silvered, collimating mirrors, whose focal length is equal to the distance from the mirror to the grating and/or the slit.

A two inch square replica grating, blazed at one micron, was used. To take advantage of this blaze angle, all visible absorption spectra, 400-700 mμ, were studied in the second order. In all infared studies, 700-1200 mμ, the first order was used.

The spectrograph was equipped with a parallel jaw slit, which could be opened reproducibly to any desired width. The settings used in this study, between 0.04 and 0.07 mm, were found to give no appreciable line broadening to low pressure helium arc lines.

The camera uses standard 4 X 5 inch spectrographic plates. It has a two component, air spaced lens system with a focal length of 15 cm, and the aperture variable from f:2.5 to f:7.7. For these studies, a setting of f:2.5 was used to take fullest advantage of the light available at the grating. The camera construction allowed five seperate exposures on each plate.

For each spectral region studied, appropriate Corning glass filters were used to remove overlapping orders and undesired wavelengths. Generally, for each study, a filter was chosen which removed all light of shorter wavelength than the region under study.

A low pressure helium arc was used for calibration purposes, the spectrum of which was photographed on each plate beside the absorption spectrum under study. This arc generally put six or seven of the more intense helium lines on the plate, the exposure time having been short enough to omit the less intense lines. Since a grating spectrograph gives a linear dispersion, the position of a given spectral feature can be accurately interpolated, once the spacing of the various helium lines is determined.

Two presentations are possible with this spectrograph. The normal presentation used in most of these studies produces resolution of 5 to 10 cm^{-1} at 18,000 cm^{-1}. A second, high resolution presentation is available which offers three times this resolution. This second presentation was not used, since the first gives generally adequate dispersion, 3 mμ per millimeter on the plate, for these studies. also, since the dispersion of the second presentation is so great, only a small portion of the spectrum can be photographed on one plate.

Kodak Spectrographic plates were used throughout this study. The first of these, 103a-F, has an effective wavelength range of 400-700 mμ. The second, 1-N, is useful for the 700-900 mμ region. Since this second plate type is considerably slower than the first, these plates were hypersensitized by washing with water and drying with methanol before use. This hypersensitization increased the speed of the 1-N plates to about that of the 103a-F plates.

Standard development and fixing techniques were followed. The plates were developed by four minutes of continuous agitation in Kodak D-19 developer at 20°C followed by a thirty second, running water rinse. They were fixed by ten minutes of continuous agitation in Kodak Acid Fixer at 20°C followed by a final thirty minute, running water rinse.

The light source used for the absorption studies was a Westinghouse 150 watt, self focusing, tungsten projector lamp. This was enclosed in a box containing a cooling blower. No attempt was made to further focus the lamp, since ample intensity was obtained without further focusing. A ground glass screen was placed between the lamp and the crystal to render the light striking all parts of the crystal uniform in intensity.

The lamp was operated through a Variac at 100 volts. Using a Variac to turn the light on and off avoided the large initial surge of power through the lamp with a resultant shortening of the life of the lamp. Since a tungsten lamp emits a great deal more intensity in the long wavelength visible than in the short, it was found necessary to place a solution of ferrous ammonium sulfate (120 g/l $Fe(NH_4)_2(SO_4)_2$ in 2% sulfuric acid in a cell 2.5 cm thick) in the light path to reduce the intensity of the longer wavelength visible light to approximately that of the shorter wavelength visible light.

For the polarization studies, a Wollaston, double refracting, polarizing prism was introduced into the light path inside the spectrograph. This prism dispersed the beam into two parallel beams, which had their respective electric vectors ninety degrees apart. Since one of the beams was parallel and one perpendicular to the molecular C_3 axis, the crystal having been mounted in this manner, studies of the polarized absorption spectrum of the crystal were possible. For these studies, the crystal was mounted with the molecular C_3 axis perpendicular to the propagation direction of the irradiating light and parallel to one of the polarization vectors of the Wollaston prism.

Using this experimental set-up, the crystals' absorption spectra, either polarized or unpolarized, were photographed at room temperature, liquid nitrogen temperature (77°K) and, where the liquid nitrogen photograph indicated possible sharpening of structural features, at liquid helium temperature (4.2°K). The results of these studies are given and discussed in the following section.

RESULTS AND INTERPRETATION

Since the interpretation of the optical spectrum of chromium (III) tris-acetylacetonate is based on Sugano and Tanabe's interpretation[7] of the ruby spectrum, both the spectrum and the energy level diagrams for the latter are reproduced here. For their calculations, Sugano and Tanabe assumed a field having C_{3v} symmetry. This is the symmetry of the oxygen atoms surrounding the Cr (III) ion in ruby, as has been shown by Wykoff.[10] Deutschbein[11] has shown that no appreciable sharpening of the spectral features is observed at temperatures below $77^{\circ}K$, so studies of ruby have generally been carried out at this temperature.

The energy level diagrams shown in Figure 3 are constructed from Sugano and Tanabe's work and are intended to show only the splitting of the various atomic states. They are not intended to be quantitative with regard to the exact energy of each level, which can be given only as a function of several parameters, but to merely indicate the relative energy of each level. It should be noted that their calculations indicated that the quartet levels are split primarily by the cubic and trigonal components of the field, while the doublet levels are split by the cubic field and by spin-orbit coupling combined with the trigonal field.

Fig. 2

ABSORPTION SPECTRUM OF Cr (III) IN CORUNDUM, 77°K. (McClure[6])

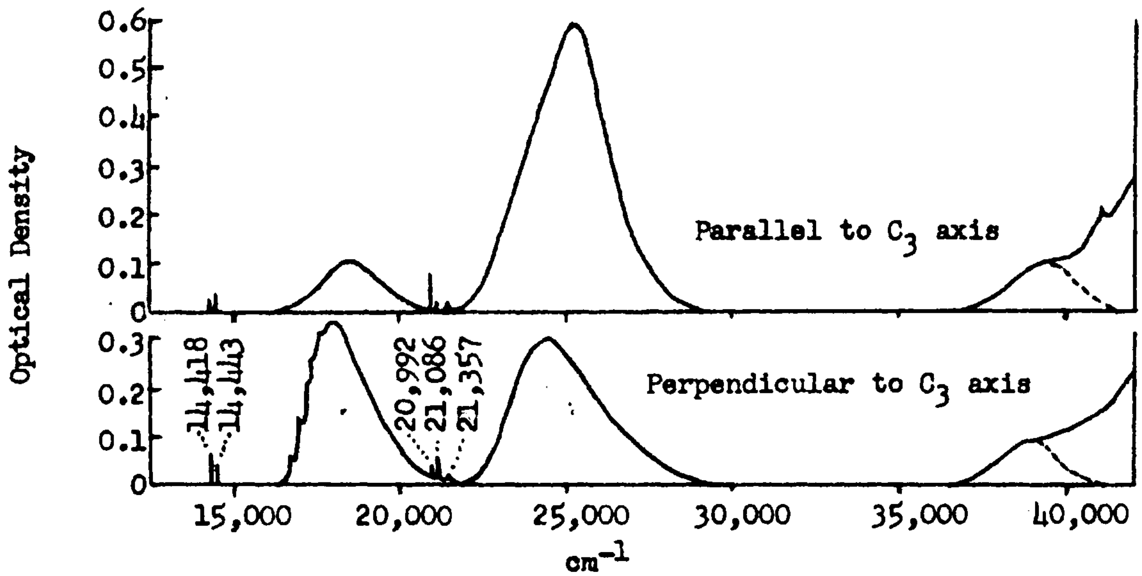

Fig. 3

ENERGY LEVEL DIAGRAMS FOR Cr (III) IN CORUNDUM

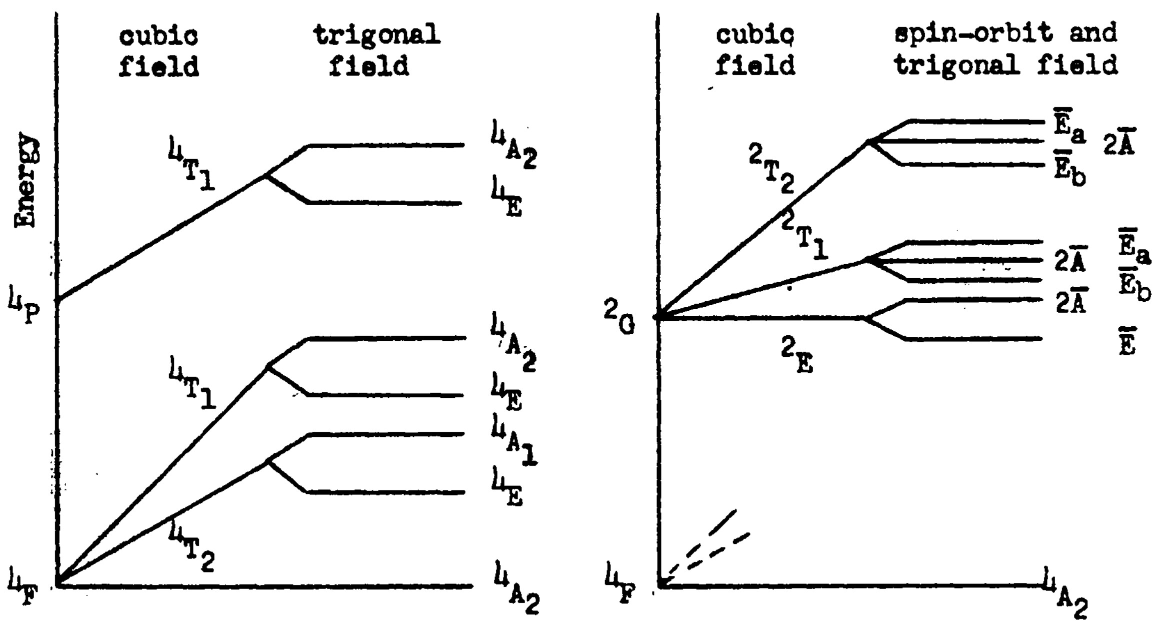

In this work, the ruby spectrum was studied merely to verify the validity of the experimental techniques used. The portions of the spectrum studied are shown in Figures 4 and 5.

It should be noted that good agreement is obtained in the polarization ratios of the intercombination lines at 14,418 and 14,443 cm^{-1} and at 20,992, 21,086 and 21,357 cm^{-1}, as well as in the vibrational structure on the lowest energy pair of bands at 18,000 cm^{-1}. It should be also noted that, in the region around 14,300 cm^{-1}, many lines, of lesser intensity than the two main lines, appear. These have been observed[10] by previous workers, although no good explanation for them has been offered. It should also be noted that an intense line occurs in this work at 14,462 cm^{-1} in the parallel polarization, which is not observed in the perpendicular polarization. This line has not been reported previously, although it has undoubtedly been observed.

One other feature of interest observed here is the structure at 14,870 and 15,050 cm^{-1}. Ford[12] has observed structure in this region, using a Perkin Elmer Spectrocord, and has assigned this to lattice vibrations. No attempt will be made in this thesis to further elucidate this structure.

The assignment of the features of the ruby spectrum by Sugano and Tanabe is given in Table 1. These assignments were verified by Sugano and Tsujikawa,[13] who studied the Zeeman splitting of the intercombination (doublet$\leftarrow$quartet) lines under the action of

Fig. 4

ABSORPTION SPECTRUM OF Cr (III) IN CORUNDUM

AT 77°K, 660-700 mμ (this work)

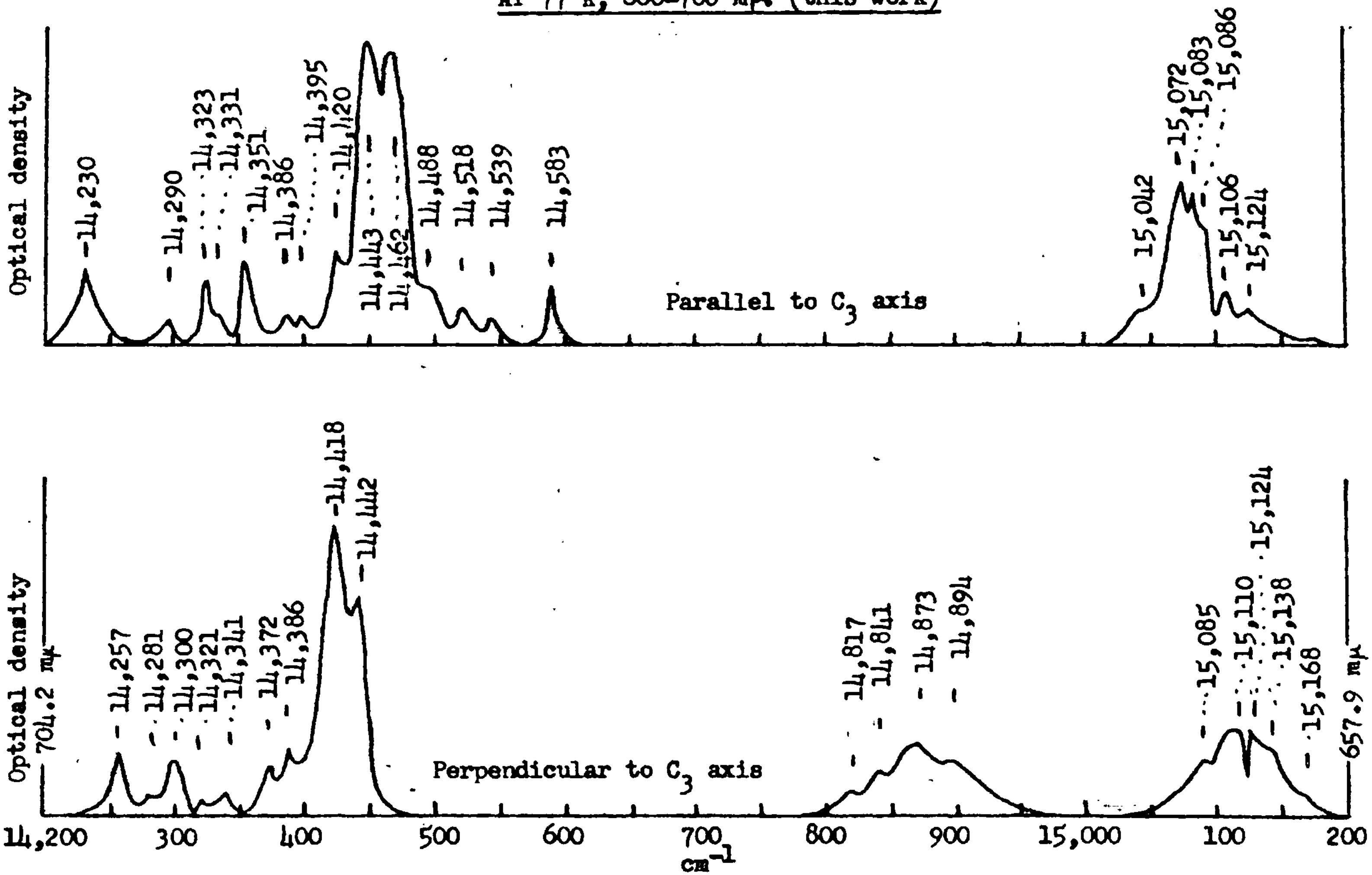

Fig. 5

ABSORPTION SPECTRUM OF Cr (III) IN CORUNDUM

AT 77°K, 450-630 mμ (this work)

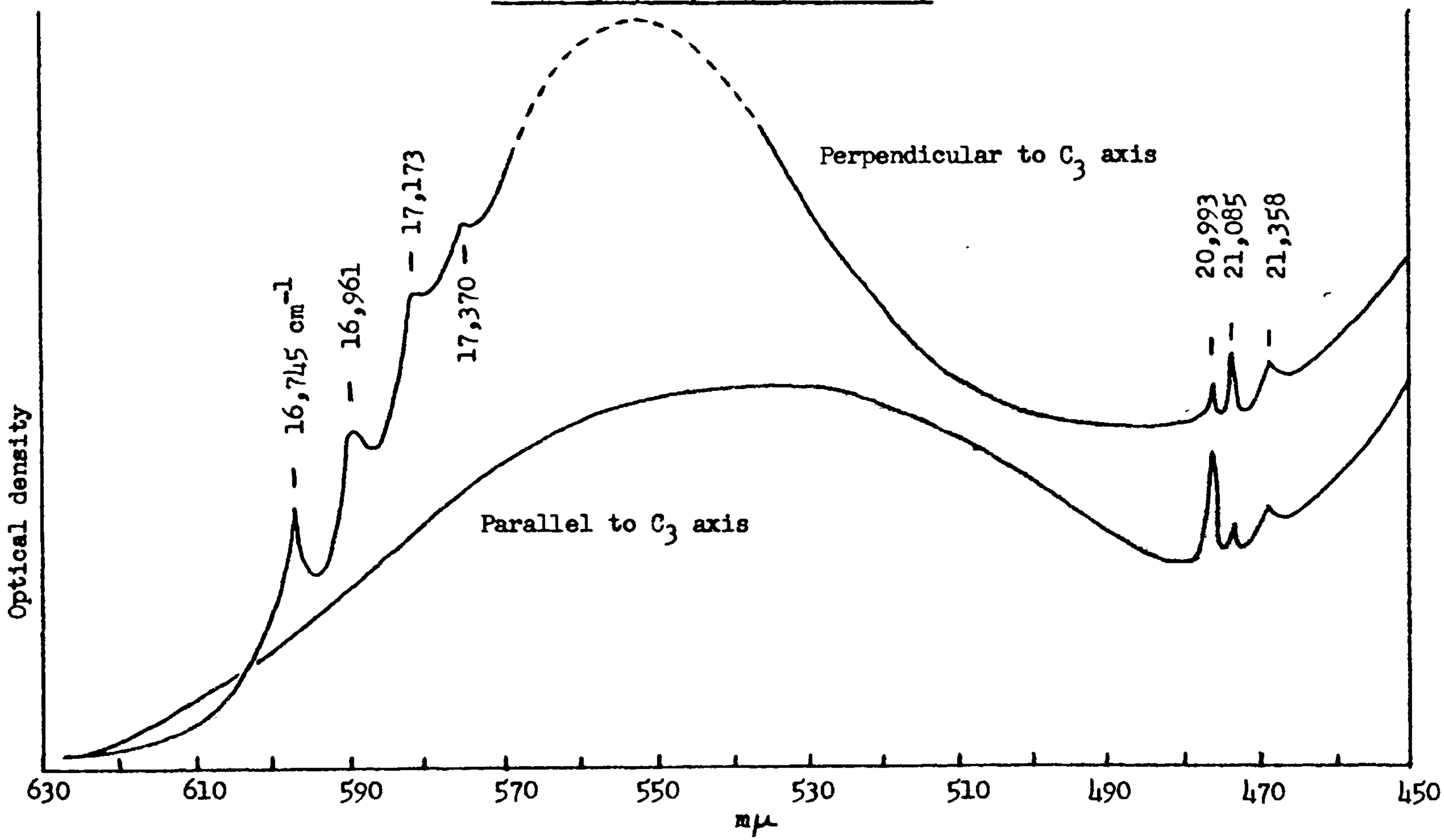

a 24,000 gauss magnetic field. They calculated the Zeeman splitting for each transition on the basis of the assignments made by Sugano and Tanabe, and found that the experimentally observed splitting for the various intercombination lines agreed with their predicted values.

Table 1

ASSIGNMENT OF SPECTRAL FEATURES OF THE RUBY (Sugano and Tanabe[7])

Position	Polarization	Assignment
~18,500 cm^{-1} (B)*	perpendicular	$^4E\ (^4T_2) \leftarrow\ ^4A_2$
	parallel	$^4A_1(^4T_2) \leftarrow\ ^4A_2$
~24,000 cm^{-1} (B)	perpendicular	$^4E\ (^4T_1) \leftarrow\ ^4A_2$
	parallel	$^4A_2(^4T_1) \leftarrow\ ^4A_2$
~38,000 cm^{-1} (B)	perpendicular	$^4E\ (^4P) \leftarrow\ ^4A_2$
	parallel	$^4A_2(^4P) \leftarrow\ ^4A_2$
14,418 cm^{-1} (L)	perpendicular	$\bar{E}\ (^2E) \leftarrow\ ^4A_2$
14,443 cm^{-1} (L)	parallel	$2\bar{A}\ (^2E) \leftarrow\ ^4A_2$
20,992 cm^{-1} (L)	parallel	$2\bar{A}\ (^2T_2) \leftarrow\ ^4A_2$
21,086 cm^{-1} (L)	perpendicular	$\bar{E}_a(^2T_2) \leftarrow\ ^4A_2$

* (B) and (L) mean band and line respectively

It should be noted that the line at 21,357 cm^{-1} has not been assigned on the basis of the above energy level diagram. On the basis of Sugano and Tanabe's work, this line does not appear to be the transition $\bar{E}_b(^2T_2) \leftarrow {}^4A_2$, since their energy level diagram places the energy of the $\bar{E}_b$ state below that of the other two components of $^2T_2$.

However, Sugano and Peter[14] recently recalculated the splitting for ruby, including in this calculation the effect of configurational mixing of higher energy states with the states originally considered. This effect was neglected in the calculations of Sugano and Tanabe. The most significant contribution of this calculation was to place the energy of the $\bar{E}_b$ level above that of the $\bar{E}_a(^2T_2)$.

On the basis of this new calculation, they tentatively assign the line observed at 21,357 cm^{-1} in ruby to the transition $\bar{E}_b(^2T_2) \leftarrow {}^4A_2$. Unfortunately, Sugano and Tsujikawa's[13] Zeeman studies were not able to verify this assignment, since this 21,357 cm^{-1} line is too broad to allow observation of its Zeeman splitting. This line does not exhibit the extreme polarization Sugano and Tanabe predicted for the transition to which this line is now assigned, but it does appear slightly more intense in the parallel polarization than in the perpendicular, which is as predicted. No mention of this inconsistency was made by Sugano and Peter.

It should be noted that transitions to the components of the $^2T_1$ state have not been identified in the ruby spectrum. Sugano and Tanabe predicted that this state should split, under the action of the trigonal field and spin-orbit coupling, into three states, whose spacing and polarization intensities should be as shown in Figure 6. Low[15] has reported three lines at 14,795, 14,950 and 15,178 cm^{-1}, which he assigns tentatively to the transitions:

$\bar{E}_a(^2T_1) \leftarrow {}^4A_2$ for the 15,178 cm^{-1} line

$2\bar{A}(^2T_1) \leftarrow {}^4A_2$ for the 14,950 cm^{-1} line

$\bar{E}_b(^2T_1) \leftarrow {}^4A_2$ for the 14,795 cm^{-1} line.

His spectrum is reproduced in Figure 7. It should be noted that these lines are very weak and do not agree with the polarizations or the spacing predicted for these transitions by Sugano and Tanabe. Since no experimental details were given by Low, it is not known how valid his assignments may be. The author of this thesis prefers to wait until Low's work is verified before accepting these assignments.

From the above discussion, we see that most of the features of the ruby spectrum can be satisfactorily explained by crystal field theory, with the addition of spin-orbit coupling effects.

We shall now attempt to interpret the spectrum of chromium (III) tris-acetylacetonate within the framework of the same theoretical treatment.

The chromium (III) tris-acetylacetonate molecule belongs to the point group symmetry D_3 and the crystal field surrounding the central ion is primarily cubic, due to the six oxygen atoms of the ligands, which form a regular octahedron about this ion. In addition to this cubic field, there is a strong trigonal field[9] whose origin is at present unknown.

Fig. 6

RELATIVE ENERGIES OF THE SPLIT COMPONENTS

OF THE $^2T_1$ STATE FOR RUBY

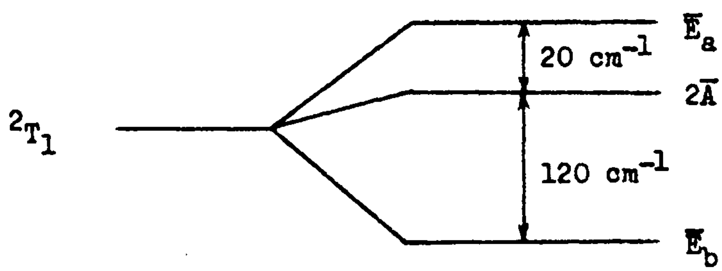

Fig. 7

ABSORPTION SPECTRUM OF RUBY, 650-700 mμ. (Low)

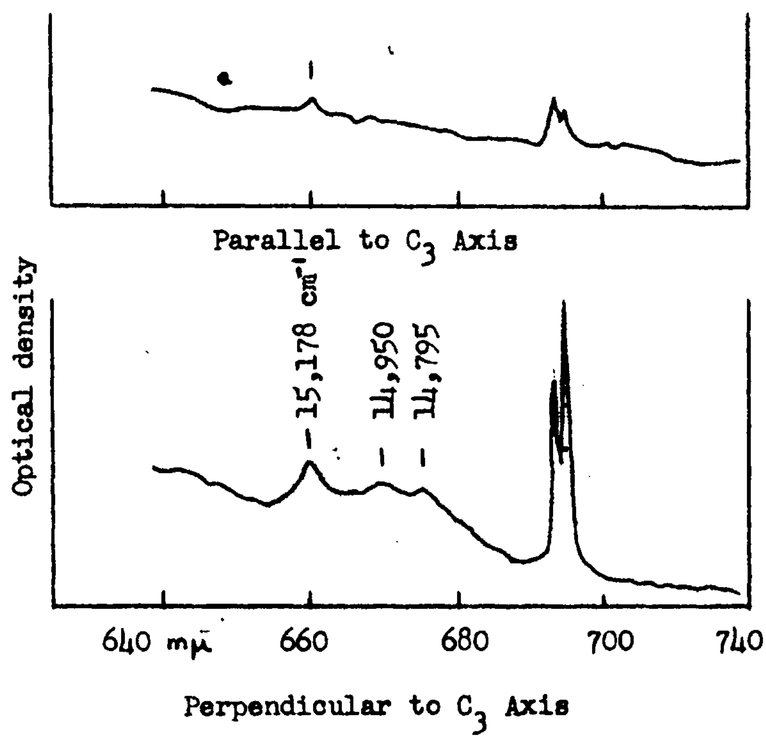

Singer,[9] who first postulated this field, to explain his EPR measurements on crystalline $Cr(AcA)_3$, showed that the interaction energy of this trigonal field with the Cr (III) ion is considerably larger than would be predicted on the basis of the molecular structure. Jarrett[16] offers two possible explanations for this field. The first is the existence of a dipole moment for the entire ligand. However, as he states, it is doubtful if this dipole could be of sufficient magnitude to create a trigonal field as strong as is observed. His second possible explanation is the effect of π bonding between the p orbital of the oxygen atoms and the t_{2g} orbitals of the central ion on these t_{2g} orbitals, which could presumably create a trigonal field by altering the electron distribution in these orbitals. The exact cause of this field is still unknown, however.

The significant point here is that the splitting pattern produced by a field of D_3 symmetry should be the same as that produced by a C_{3v} field. Since the splitting pattern is the same for both symmetry species, we should be able to interpret the $Cr(AcA)_3$ spectrum, whose field probably has D_3 symmetry, by analogy to the ruby spectrum, whose field has C_{3v} symmetry. In each case, we expect the same splitting pattern.

The splitting of the doublet levels may be less in $Cr(AcA)_3$ than in ruby, since this is partly due to spin-orbit coupling and it is known that an increase in the covalent nature of a bond will decrease the importance of this coupling. This effect, if observed, will change only the quantitative splitting of the intercombination lines, however, and will have no effect on the essential qualitative features of the energy level diagram.

Singer[9] offers as proof of the large degree of covalency of chromium (III) complexes the following;

1. The slow exchange of the ligands of chromium (III) chelates and complexes with ligand molecules in solution. Presumably, if the bonding were largely ionic, a rapid exchange would be noted.

2. The slow rate of racemization of optically active chromium (III) complexes. Here again, ionic bonding would predict rapid racemization.

Quantitative application of the ruby energy level diagram to $Cr(AcA)_3$ cannot be fully justified. However, as will be shown, the chelate spectrum can be semi-quantitatively interpreted using this energy level diagram. The discrepencies noted can be easily rationalized.

The optical spectrum of $Cr(AcA)_3$ is reproduced in Figures 8 and 9. It will be noted that only a portion of this spectrum is polarized. We have not yet succeeded in obtaining a polarized spectrum of the 500-700 mμ region. It is hoped that polarization studies of this region can be made to verify the tentative assignments made in this thesis.

To determine the orientation of the molecular C_3 axis with respect to the crystallographic axes, Singer[9] used $Cr(AcA)_3$ crystals,

Fig. 8

ABSORPTION SPECTRUM OF $Cr(AcA)_3$ AT 77°K, 675–780 mμ

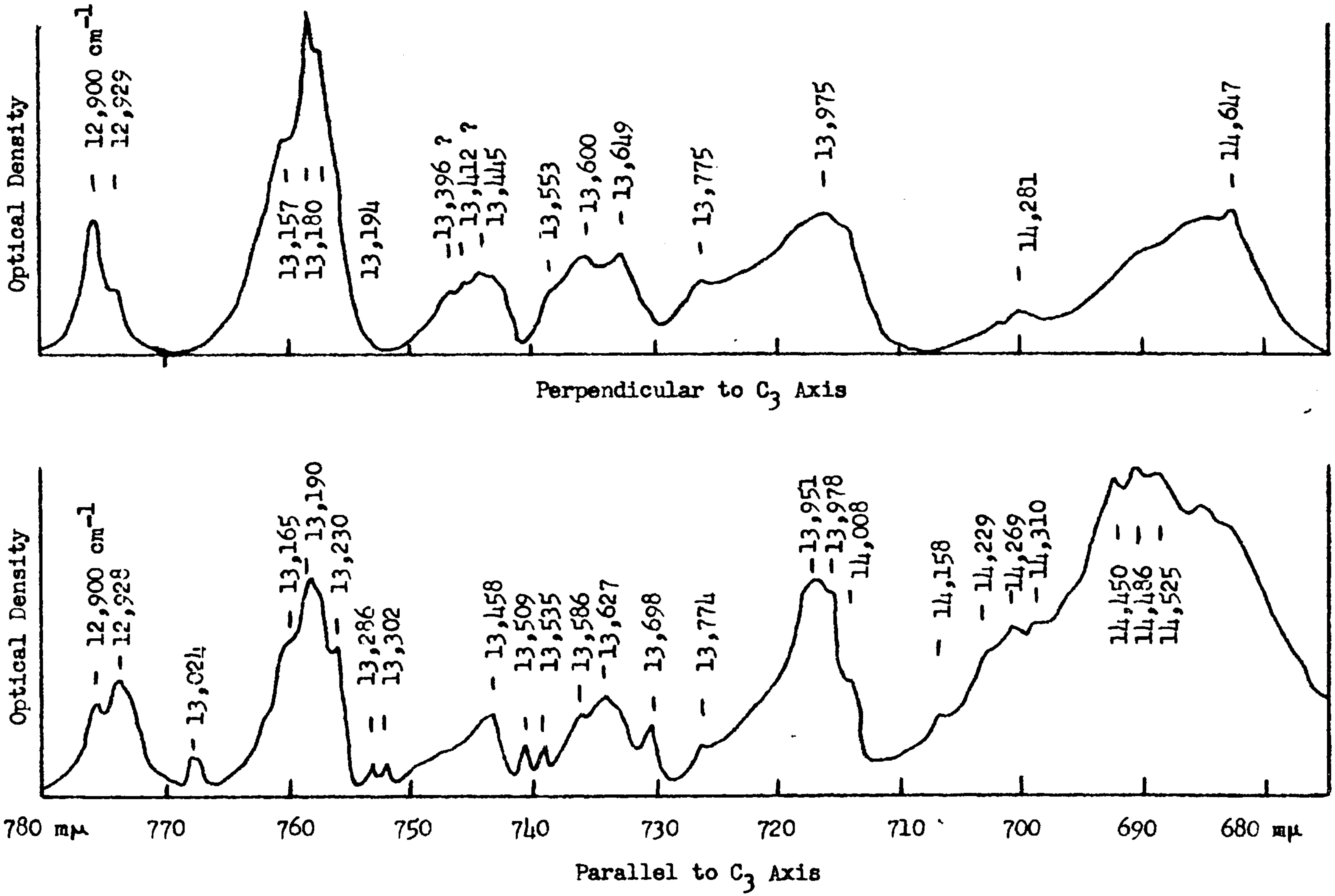

Fig. 9

ABSORPTION SPECTRUM OF $Cr(AcA)_3$, 490–590 mμ

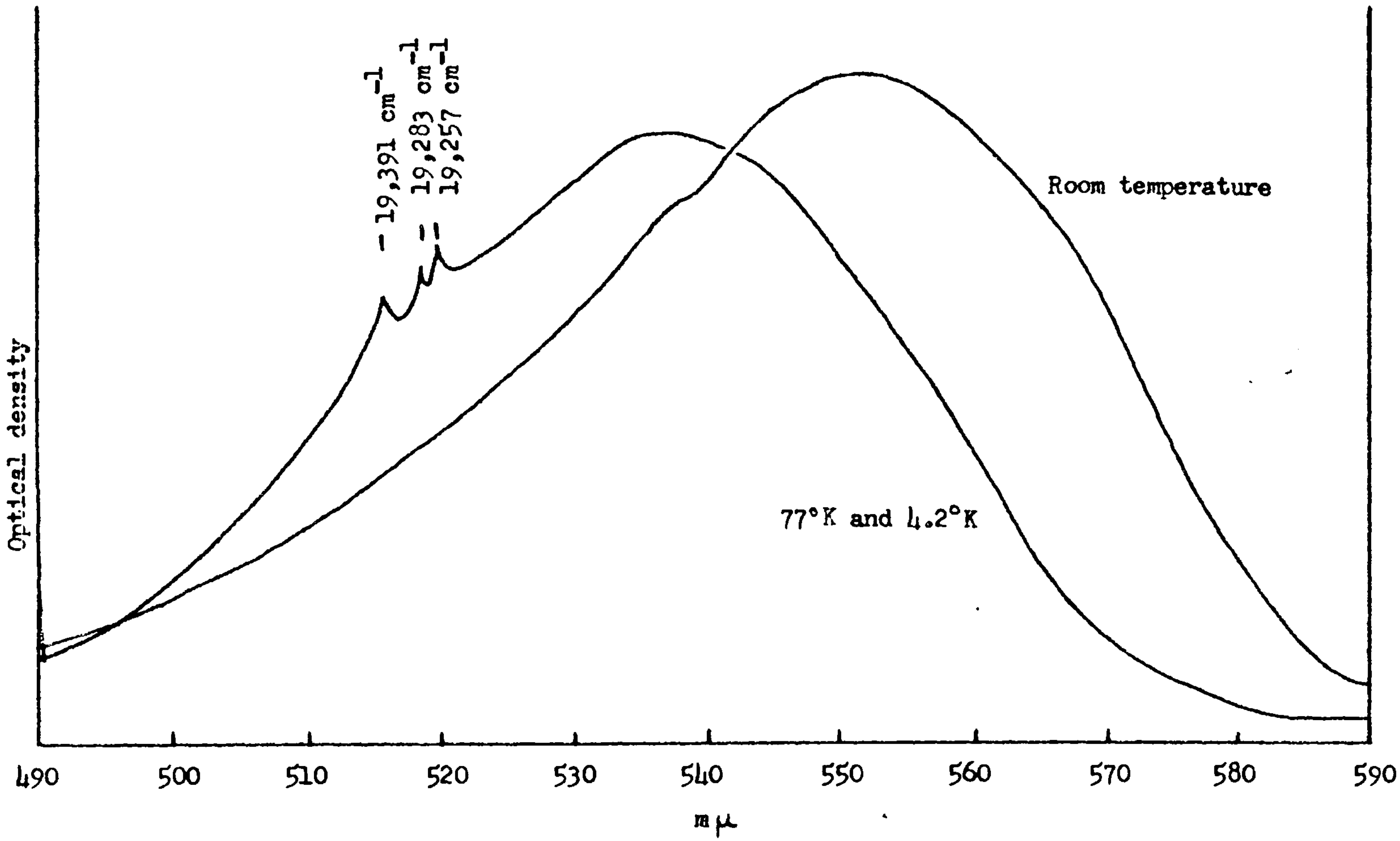

oriented in a magnetic field for ground state Zeeman studies. These studies indicated that the molecular C_3 axis lay at an angle of $31 \pm 1°$ from the crystallographic b axis. His studies could not, however, determine the exact location of this molecular axis, but merely placed it on a cone about the b axis.

Due to the uncertainty of this placement, we merely oriented the crystal with respect to the crystallographic b axis, whose location was determined by Dr. R. L. DuBois, of the University of Arizona. The orientation of the crystallographic axes is shown in Figure 10. The crystal shape shown is that obtained when the crystal is grown by the methods described above. The relative dimensions of the crystal, in the directions shown, are approximately 10:20:1 for the a, b and c directions respectively.

Fig. 10

LOCATION OF CRYSTALLOGRAPHIC AXES IN $Cr(AcA)_3$ CRYSTALS

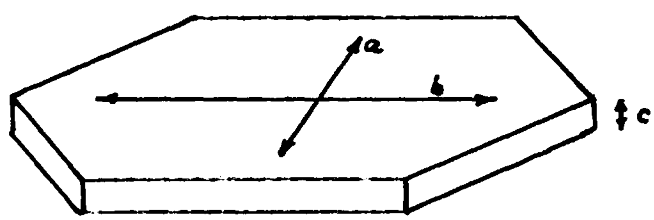

Using crystals oriented in this manner, it was not possible to determine the exact intensity ratios of a given transition in the different polarizations, but polarization trends are observable. These trends are sufficient to allow tentative assignments. In the polarized spectrum determinations, the crystal was mounted with the crystallographic a axis parallel to the propagation direction of the source light and the b axis parallel to one of the vibration directions of the Wollaston prism.

There are several features of the unpolarized (500–700 mμ) region which are of interest. The broad absorption band, having its maximum at about 535 mμ at 77°K and 4.2°K is undoubtedly the (components of $^4T_2$) $\leftarrow$ $^4A_2$ transition, observed at 18,500 cm^{-1} in ruby. Chakravorty and Basu[17] reported a study of the optical anisotropy of this band at room temperature. Their spectrum is reproduced in Figure 11.

Fig. 11

PARTIAL SPECTRUM OF $Cr(AcA)_3$ AT ROOM TEMPERATURE

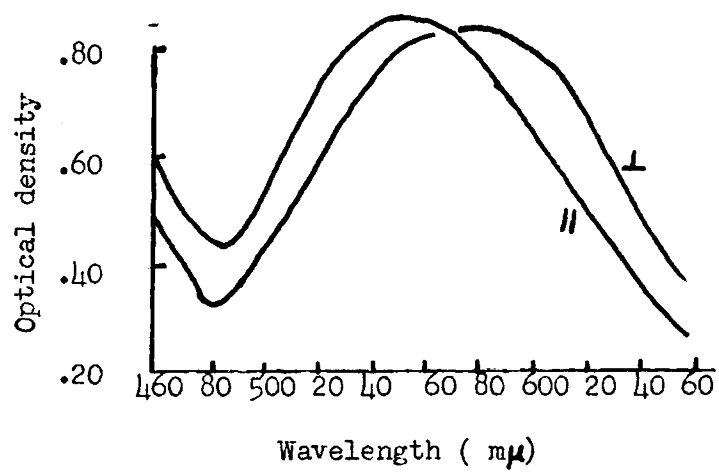

No experimental details were given, so it is not known exactly how their crystal was oriented. They did report the polarizations as parallel and perpendicular to the "long axis of the crystal". It must be assumed that this long axis corresponds to the b axis of the crystal, which, as was seen previously, is normally the longest dimension of the crystal. Since their work was done at room temperature, they did not observe the fine structure seen in the low temperature tracings of Figure 9.

The position of maximum absorption observed by them is at the same wavelength observed by this author at room temperature. As is expected, there is a considerable shift of the maximum with a decrease in temperature. This shift is caused by a thermal depopulation of the excited vibrational levels of the ground state, thus removing the low energy vibronic transitions from these levels.

The significant feature of their work is that the two polarizations show the higher energy transition is polarized parallel to the molecular C_3 axis, which is as assigned in the ruby (See Table 1). Thus, it is entirely reasonable to assign these two bands to the split components of the $^4T_2$ state. The transitions observed are then:

Parallel polarization $^4E \leftarrow {}^4A_2$ (555 mμ)

Perpendicular polarization $^4A_1 \leftarrow {}^4A_2$ (585 mμ).

Another feature to be observed in this region is the complete absence of fine structure on the low energy side of these bands, even at 4.2°K. In the ruby spectrum, five distinct peaks are observed. The spacing of these peaks is about 200 cm^{-1}, which agrees with the ground state vibrational spacing obtained by Krishman[18] in the infared, 194 cm^{-1}. It has been assumed, therefore, that these peaks are vibrational structure of the excited state.

The absence of vibrational structure in $Cr(AcA)_3$ is probably due to the complexity of the ligand, which allows many vibrations of similar energy within the ligand. Hence, the sharp vibrational features of the chromium-oxygen bond, observed in ruby, are obscured by a superposition of many vibrations within the ligand of $Cr(AcA)_3$.

To test this hypothesis, the corresponding band in cobalt (III) tris-acetylacetonate was examined at room temperature, 77°K and 4.2°K. This band, unpolarized, for $Co(AcA)_3$ is shown in Figure 12. It should be noted that no vibrational structure appears here, even though it has been observed in Co (III) suspended in aluminum oxide.[19] Since this situation is completely analagous to the Cr (III), it may be safely assumed that the complexity of the ligand is responsible for this absence of structure.

Although similar vibrational structure has been reported for V (III),[20] Mn (III),[19] and Ni (III)[19] in aluminum oxide, the acetylacetonate chelates of these ions were not examined for such structure, due to the absence of this in the two chelates studied.

The most significant feature of the unpolarized spectrum of $Cr(AcA)_3$ is the occurence of three sharp lines in the higher energy

Fig. 12

ABSORPTION SPECTRUM OF $Co(AcA)_3$, 550–630 mμ

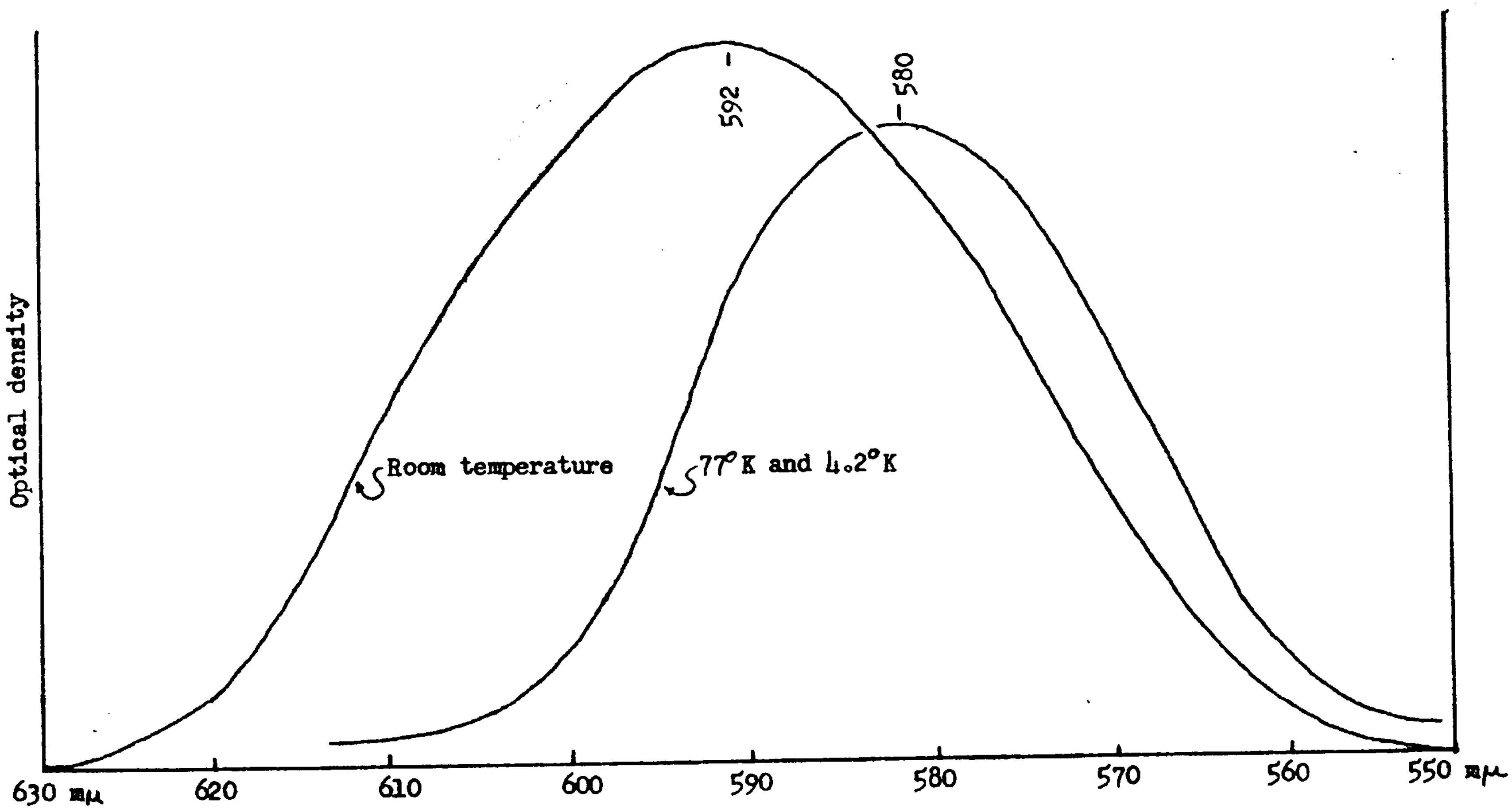

region of the broad absorption band. Although the optical anisotropy of these lines has not yet been determined, their spacing is directly related to the spacing of the (split components of $^2T_2$) $\leftarrow$ $^4A_2$ lines observed in ruby near 21,000 cm^{-1}. The spacing of the lines for these two materials is shown in Figure 13.

Fig. 13

COMPARISON OF SPACING OF 21,000 cm^{-1} LINES OF RUBY AND 19,000 cm^{-1} LINES OF $Cr(AcA)_3$

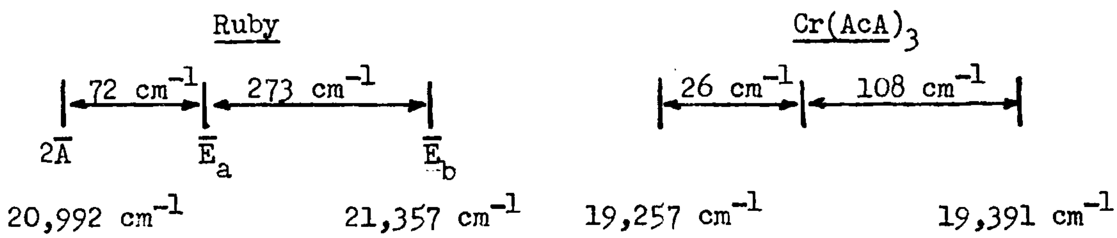

Two features of this comparison are important, both of which may be explained by the same assumption. The first of these is the same ratio of spacing in both ruby and $Cr(AcA)_3$; 1:4 for the ruby and 1:4 for the $Cr(AcA)_3$. The absolute spacing for $Cr(AcA)_3$ is only about one third as large as that of the ruby, but since this splitting is partly due to spin-orbit coupling, we would expect the spacing to decrease with a decrease in spin-orbit coupling. Since we assume a greater degree of covalency in $Cr(AcA)_3$ than in ruby, we expect less spin-orbit coupling in the former and hence less splitting. The ratio of the spacing of the lines should remain nearly constant in the two materials, however.

The second feature to be observed is the shift of these lines to a lower energy in $Cr(AcA)_3$ by about 1500 cm^{-1}. This shift is also expected if we postulate a greater degree of covalency of bonding in $Cr(AcA)_3$ than in ruby, since this bonding will reduce the energy of the original ^2G spectroscopic level, from which these excited states originate.

The above facts, coupled with the absence of any other lines in this spectral region, indicate that these lines may be assigned to the transitions:

$2\bar{A}\ (^2T_2) \leftarrow {^4A_2}$ for the 19,257 cm^{-1} line

$\bar{E}_a\ (^2T_2) \leftarrow {^4A_2}$ for the 19,283 cm^{-1} line

$\bar{E}_b\ (^2T_2) \leftarrow {^4A_2}$ for the 19,391 cm^{-1} line.

These predictions should be verified by both a study of the optical anisotropy of these lines and by a study of their Zeeman splitting. If these predictions are correct, both should be similar to the values obtained by Sugano and Tsujikawa[13] for the ruby.

A second portion of the $Cr(AcA)_3$ spectrum is also of interest. In Figure 8 is reproduced the the spectrum of $Cr(AcA)_3$ in the region from 700 to 900 mμ in both polarizations. It should be noted that considerably more detail is observed in the parallel polarization than in the perpendicular and that the intensity of several of the bands shows a dependence on the polarization direction. These facts indicate that the crystal orientation is good enough to allow observation of polarization trends.

The feature of particular interest here is the optical anisotropy of the band at 12,900 cm^{-1}. This band has not been resolved into two distinct components, due to concentration broadening, but an attempt to do so is now being made. At the present time, however, it does appear that this band consists of two components which are oppositely polarized. The spacing of these two components appears to be about 30 cm^{-1}, although they are not sufficiently sharp to allow exact determination of their spacing.

Here also, there are two features which should be noted. The first, and most important, is the optical anisotropy of the two components. The high energy line at 19,928 cm^{-1} appears to be more intense than the low energy line, at 12,900 cm^{-1}, in the parallel polarization and less intense in the perpendicular. The second feature of interest is that these lines are located about 1600 cm^{-1} below the 14,440 cm^{-1} intercombination lines of ruby. This is roughly the same shift observed for the high energy intercombination lines.

These lines exhibit the same optical anisotropy as the ruby intercombination lines ($\bar{E} \leftarrow {}^4A_2$ at 14,420 cm^{-1} and $2\bar{A} \leftarrow {}^4A_2$ at 14,443 cm^{-1}) and they are shifted in the same way as the previously assigned intercombination lines. Thus it seems entirely reasonable to assign these two lines of $Cr(AcA)_3$ to the transitions:

$\bar{E}$ (^2E) $\leftarrow$ $^4A_2$ for the 12,900 cm^{-1} line

$2\bar{A}$ (^2E) $\leftarrow$ $^4A_2$ for the 12,928 cm^{-1} line.

As was stated above, due to the width of these lines, it is not possible to give their exact spacing. Hence, the discrepency in the spacing of these lines relative to that of the ruby, 28 cm^{-1} vs. 24 cm^{-1} respectively, is not as serious as it may first appear.

No attempt will be made to interpret the other features of this low energy portion of the optical spectrum. This author does, however, suspect that some of the other peaks observed in the 700-780 mμ region of the $Cr(AcA)_3$ spectrum may be the components of the $^2T_1 \leftarrow {}^4A_2$ transition. Since the other two sets of intercombination lines have apparently been shifted to lower energy in $Cr(AcA)_3$, it is not unreasonable to expect that transitions to the components of the $^2T_1$ level would also be shifted to a lower energy. This shift could presumably move these lines out of the 18,000 cm^{-1} bands, where this author suspects they are in ruby, into this spectral region of $Cr(AcA)_3$.

CONCLUSIONS

In this study, an attempt has been made to tentatively assign many of the structural features of the chromium (III) tris-acetylacetonate spectrum, using the energy level diagram developed by Sugano and Tanabe for the ruby. If the assignments made in this study prove valid, it may be concluded that this diagram can be applied, at least qualitatively, to other Cr (III) chelates, having the same symmetry of field as $Cr(AcA)_3$. This diagram will furnish a valuable tool in the interpretation of these spectra.

This study has also indicated that a study of the splitting of intercombination lines and their shifting may be a valuable tool in the study of the covalency of bonding in chelates. As has been seen, the degree of covalency may be inferred qualitatively from both of these properties. It may prove possible to develop a systematic "covalency" parameter enabling one to relate these changes to the degree of covalency. This will be accomplished only after a systematic study of several related chelates whose relative covalency can be estimated independently.

It has also been seen that pure electrostatic crystal field theory is not sufficient to explain many of the features of these spectra. This is seen both in the existence of doublets and triplets for intercombination lines, which rely on spin-orbit coupling for an explanation, and in the shifts of these lines, apparently with covalent bonding character. Thus, it becomes necessary to graft several extensions onto crystal field theory to explain all the observed features of these spectra. This emphasizes that, while each theory may be quite satisfactory in its explanation of a single feature, a unified theory, capable of explaining all the features, is still not a reality.

It is significant, however, that such a large degree of success can be attained by grafting these different theories together.

SUGGESTIONS FOR FURTHER STUDY

Polarized studies of the high energy intercombination lines of $Cr(AcA)_3$ should be carried out to verify their optical anisotropy. This study would have to be performed on thin crystals (0.1 mm) at low temperatures, either 77°K or 4.2°K.

The low energy intercombination lines should be better resolved to determine more accurately their spacing and to verify their observed optical anisotropy. Both of these can be accomplished by using a high dispersion spectrograph to increase the resolution and by using dilute, mixed crystals to minimize concentration broadening.

An attempt should also be made to identify the components of the missing $^2T_1 \leftarrow {}^4A_2$ transition in $Cr(AcA)_3$. It is quite possible that this transition gives rise to one or more of the peaks observed in the 700–770 mμ region of the $Cr(AcA)_3$ spectrum. If this is true, the above mentioned techniques should resolve this peak, or these peaks, into its components.

It will also prove advantageous to study other chelates related to the acetylacetonates, whose bonding should be more or less covalent than this. This study will test the hypothesis of covalency of bonding being related to intercombination line behavior.

Two excellent ligands for this are trifluoroacetylacetone and hexafluoroacetylacetone, the Cr (III) chelates of which have been prepared by Mr. P. X. Armendarez, who will continue this project. These two chelates should be more or less covalent than the one studied here, due to the presence of highly electronegative atoms near the chelating oxygen atoms. This should reduce the negative charge on the oxygen atoms, and thus change the covalency of the metal-oxygen bonds. If the above assignments are correct, these chelates should show a difference in the splitting of the intercombination lines and in the position of these lines.

The infared spectra of these chelates could be examined to determine the relative covalency of these bonds, as it is expected that the stretching frequency of the metal-oxygen bond should reflect changes in the covalency of this bond.

LIST OF REFERENCES

1. H. A. Bethe, Ann. Physik, 3, 133 (1929).

2. Robert Schlapp and William G. Penney, Phys. Rev., 42, 666 (1932).

3. Linus Pauling, "Nature of the Chemical Bond," 2nd ed., Ithica Press, New York, 1940, pp. 93-123.

4. Leslie E. Orgel, J. Chem. Soc. (1952) 4756.

5. R. Finkelstein and J. H. Van Vleck, J. Chem. Phys., 8, 790 (1940).

6. Donald S. McClure, Solid State Physics, 9, 399 (1959).

7. Saturo Sugano and Yukito Tanabe, J. Phys. Soc. Japan, 13, 880 (1958).

8. Leslie E. Orgel, "Introduction to Transition Metal Chemistry-Ligand Field Theory," Methuen and Co., London, 1960.

9. L. S. Singer, J. Chem. Phys., 23, 379 (1955).

10. R. W. G. Wykoff, "Crystal Structures," Vol I, Interscience Publishers, New York, 1948, Chap. V, text page 4.

11. O. Deutschbein, Ann. Phys., 20, 828 (1934).

12. R. A. Ford, to be published.

13. Saturo Sugano and Ikuji Tsujikawa, J. Phys. Soc. Japan, 13, 899 (1958).

14. Saturo Sugano and M. Peter, Phys. Rev., 122, 381 (1961).

15. W. Low, J. Chem. Phys., 33, 1162 (1960).

16. H. S. Jarrett, J. Chem. Phys., 27, 1298 (1957).

17. Animesh Chakravorty and Sadhan Basu, J. Chem. Phys., 33, 1266 (1960).

18. Krishman, Proc. Indian Acad. Sci., 26A, 450 (1947).

19. Donald S. McClure, unpublished work.

20. M. H. L. Pryce and W. A. Runciman, Discussions Faraday Soc., 26, 34 (1958).